Aerothermodynamic Aspects of Shock-Interference Patterns for Shuttle Configurations during Entry

JOHN J. BERTIN* AND BRUCE W. GRAUMANN†
The University of Texas at Austin, Austin, Texas
AND
WINSTON D. GOODRICH‡
Johnson Space Center, Houston, Texas

Theme

A VITAL part of the entry aerothermodynamic environment for the Space Shuttle Orbiter is the convective heat-transfer rate in the severely perturbed shock-interference regions of the shuttle flowfield. To better understand the interactions among shock waves, shear layers, and boundary layers for simple configurations in hypersonic flow has been the goal of many investigators. The purpose of the present study is to create a better understanding of these interactions for complex three-dimensional flowfields produced by both straight-wing and delta-wing shuttle orbiter configurations. This objective is accomplished with the aid of an experimental study that considers the influence of configuration geometry, angle of attack, Mach number, and Reynolds number on the shuttle flowfield. These data are used to create and verify shock-interference models which are applicable in regions of flowfield perturbations caused by the fuselage-shock: wing-shock interactions.

Contents

It has been observed that hypersonic vehicles can experience severe damage due to locally high heating rates generated when the bow shock wave of the vehicle intersects the shock wave generated by the leading edge of a wing or fin. Many of the investigations of the related shock-interference problems have employed a shock generator to generate the incident, or "bow," shock wave and a fin with a hemicylindrical leading edge to represent the wing. As the angle between the shock-generator surface and the cylinder axis decreases, a distinct change occurs in the structure of the flowfield created by the intersecting waves. The investigation of Hiers and Loubsky[1] provide valuable information about these shock-interference patterns. However, it was not until the systematic investigation of Edney,[2] that accurate flow models of the shock-interference patterns were established as a function of the sweep angle.

Edney stated that six types of shock-interference patterns were possible for swept cylinders with only three of these patterns being probable with positive sweep. Sketches of these patterns are reproduced in Ref. 3. The effective sweep angles obtained for swept cylinders mounted on a shock generator are presented in Fig. 1. as a function of angle of attack and of geometric sweep angle (for zero angle of attack). The effective sweep angle was calculated as a function of alpha using

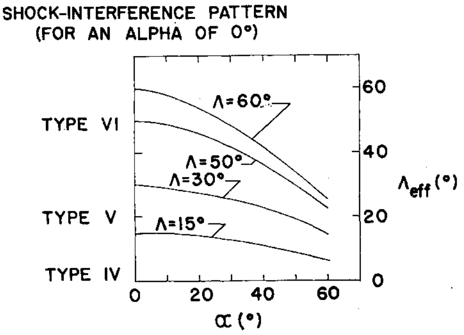

Fig. 1 Effective sweep angle as a function of angle of attack.

$$\cos \Lambda_{eff} = (\tan^2 \Lambda \sin^2 \alpha + 1)^{0.5} \cos \Lambda$$

The approximate locations of the three types of interference patterns for varying sweep angles (at zero angle of attack) are also indicated on the figure. Marked differences between effective sweep-angle occur only for highly swept wings at high angles of attack.

An experimental program was conducted to test this extrapolation of Edney's interaction model types for use on complex shuttle orbiter configurations experiencing shock-induced interactions. The experimental programs included freestream Mach numbers from 8 to 17 with freestream Reynolds numbers from 0.8×10^6/ft to 1.3×10^7/ft. Data were obtained in several different facilities for both straight-wing orbiters and delta-wing orbiters. Heat transfer, surface pressure, and flow-visualization data were used to construct flow models for the shock-interference patterns. These experimental flow models have been interpreted in terms of models established for the shock-shock interaction for swept cylinders mounted on a shock generator and are described in detail in Ref. 3.

A sketch of the shock-interference pattern is presented in Fig. 2 for the highly swept delta-wing configurations. The data indicated that the intersection geometry between the bow generated shock wave and the wing-generated shock wave and the associated expansion waves correspond to the Type VI pattern. The interaction of the expansion waves with the wing boundary layer produced no discernible increase in the wing leading-edge heat-transfer rates. This is a favorable indication for the shuttle design, since the Type VI interaction covers a range of effective wing leading-edge sweep angles. However, the data also indicated flowfield perturbations not associated with the Type VI pattern. Locally high heating rates occurred due to shock waves generated at the leading edge of the wing-root fairing and to a shear layer formed along the curved intersection of the

Presented as Paper 73-238 at the AIAA 11th Aerospace Sciences Meeting, Washington, D. C., January 10–12, 1973; submitted January 15, 1973; synoptic received April 23, 1973; revision received May, 15, 1971. Full paper available from AIAA Library, 750 Third Avenue, New York, N.Y. 10017. Price Microfiche, $1.00; hard copy, $5.00. **Order must be accompanied by remittance.** This work was supported by the NASA Manned Spacecraft Center, Contract NAS-9-11082.

Index category: Jets, Wakes, and Viscid-Inviscid Flow Interaction.

* Associate Professor, Department of Aerospace Engineering and Engineering Mechanics. Member AIAA.

† Research Assistant, Department of Aerospace Engineering and Engineering Mechanics. Member AIAA.

‡ Aerospace Technologist.

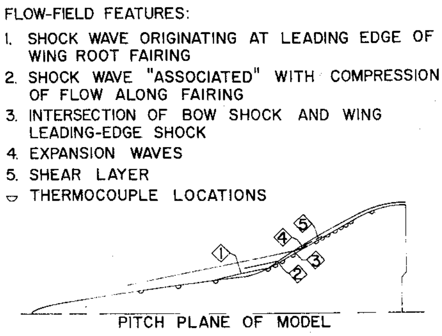

Fig. 2 Proposed shock-interference pattern for a delta-wing orbiter (with 60° sweep) at $\alpha = 0°$.

fuselage-shock surface with the wing-shock surface. The strength of these perturbations was a function of local geometry and of angle of attack.

Based on the effective sweep-angle relation presented in Fig. 1, one would expect that the "straight-wing" configurations would generate a Type V interference pattern. A schlieren photograph and an interpretive sketch of the shock-interference pattern is presented in Fig. 3 for a straight-wing configuration with $\Lambda = 15°$. The data indicate the existence of the transmitted shock wave, the shear layer, and the jet, which characterize the Type V interference pattern. Also included is a sketch of the darkened patterns of surface degradation which were observed on the wing surface of painted models.

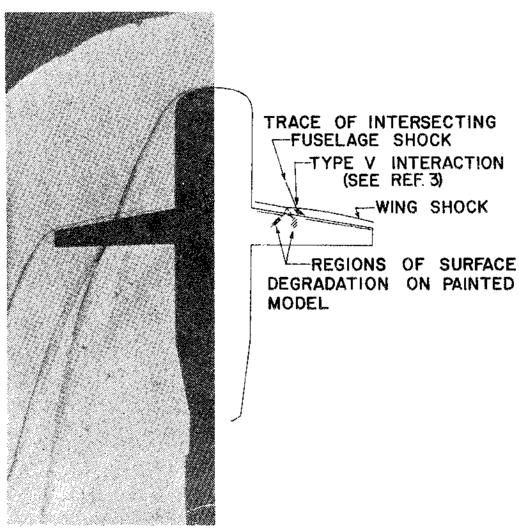

Fig. 3 Flowfield of a straight-wing orbiter (with 15° sweep) at $\alpha = 50°$.

At very high angles of attack, the shock-wave envelope changes from a surface consisting of two identifiable component waves to a single, complex surface. The value of alpha at which this change occurs appears to be greater for the straight-wing configurations and is affected by many geometric parameters including: the wing planform area, the leading-edge sweep, wing offset and dihedral, and the curvature of the windward surface of the fuselage.

The Edney Type IV interaction was not observed for the models and test conditions of this study, even at the lowest wing-leading-edge effective sweep angles. However, had the test program used additional test conditions, instrumentation, and facilities the Type IV pattern may have been observed.

Based on the data and analyses of the present study, the following conclusions are made for the configurations and test conditions of this program.

1) *Configuration geometry*: The sweep angle of the wing leading edge governs (to first order) the type of interference pattern (although inboard of the shock : shock intersection, the flowfield is sensitive to the angle of attack). The interaction between the fuselage-generated shock wave and the wing generated shock wave depends primarily on the local model geometry, i.e., that in the vicinity of the wing. The wing-root fairing has a marked effect on the heat-transfer rates over an extensive surface area.

2) *Heat transfer perturbation*: The maximum perturbation in heat transfer was only a factor of 3 which was observed for straight-wing configurations. Since the increase in the heat transfer is less for the Type VI interference pattern, the maximum perturbation measured for the delta wing was less than 2.0 for the present tests.

3) *Mach number*: For the hypersonic flow considered, there appeared to be no significant effect of Mach number. However, these data were obtained in facilities where γ was approximately 1.4, regardless of the Mach number. When applying these data to hypersonic flight, the real-gas effects are the important phenomena associated with the Mach number variation.

References

[1] Hiers, R. S. and Loubsky, W. J., "Effects on Shock-Wave Impingement on the Heat Transfer on a Cylindrical Leading Edge," TN D-3859, Feb. 1967, NASA.

[2] Edney, B., "Anomalous Heat Transfer and Pressure Distributions on Blunt Bodies at Hypersonic Speeds in the Presence of an Empinging Shock," Rept. 115, 1968, Flygtechniska Försöksanstalten, Sweden.

[3] Bertin, J. J., Graumann, B. W., and Goodrich, W. D., "Aerothermodynamic Aspects of Shock-Interference Patterns for Shuttle Configurations During Entry," AIAA Paper 73-238, Washington, D.C., 1973.